MEG/EEG Analysis of Inter-ictal Activities on Epilepsy Patients

A Thesis

SUBMITTED TO THE FACULTY OF

UNIVERSITY OF MINNESOTA

BY

Shuai Ye

IN PARTIAL FULFILLMENT OF THE REQUIREMENTS

FOR THE DEGREE OF MASTER OF SCIENCE

Advisor: Bin He

January 2018

Table of Contents

List of Tables

List of Figures

Introduction

Epilepsy is a chronic neurological disorder affecting over 65 million people in the world (3 million people in the United State) (England et al. 2012). People with epilepsy are usually treated with antiepileptic drugs (AEDs) to control their seizures. However, about 30% of these patients do not respond to the medications, and the seizure cannot be controlled even with multiple AEDs (Engel 2008; Palmini et al. 1991). Neuro-stimulation treatments could be performed in some medically resistant epilepsy patients to suppress seizures. However, even in the closed-loop responsive cortical stimulation, localizing the epileptogenic zone is important for guiding the implantation of brain stimulation leads. Surgical intervention is another option for these patients, which would also require the accurate localization of seizure onset zone (SOZ). Thus, accurate localization of the SOZ plays a critically important role in guiding the resection surgery and in directing brain stimulation (Tanaka and Stufflebeam 2014).

The criteria for defining the SOZs are far from being standardized. In short, they correspond to a compromise solution between the lesion volume as seen by imaging methods (MRI, PET, SPECT...), and the extent of inter-ictal and ictal activities as delineated by electrophysiology. In clinical setting, ictal activities could be one strong supporting evidence to help lateralize or localize seizure onset regions in epilepsy patients. However, a reliable recording of seizure data, which requires prolonged monitoring of patients for more than 48 hours, and the development of methodologies to image such a dynamic ictal process, still remain as challenges for seizure imaging. Another important biomarker could be inter-ictal activities. After Bancaud and Talairach's contributions to the concept of "Epileptogenic Zone" (Talairach and Bancaud 1973), adoption of the seizure onset area as the major criterion to define a potential surgical strategy has been progressively preferred to the localization of inter-ictal activities (Bautista et al. 1999; Hufnagel et al. 2000). The inter-ictal epileptic discharges (IEDs), which are also referred as

inter-ictal spikes, has been widely studied due to their frequent occurrence in epilepsy patients. Their generators usually overlap with the region involved in the seizure onset (Staley and Dudek 2006).

Both ictal and inter-ictal activities have been studied to localize the seizure onset zone in clinical setting. Seizures have more complicated spatiotemporal features and involve multiple brain area activating simultaneously, whereas inter-ictal spike bursts are usually relatively focal, transient events without excessive activation as no behavior abnormality associated with spikes, by definition (Staley and Dudek 2006). At the same time, it is also well-known that the irritative zone defined by peak of inter-ictal spikes does not reliably determine the minimum region of brain tissue that must be resected in order to render the patient seizure free (Marsh et al. 2010), which suggests a demand for spike propagation studies. The availability of reliable dynamic IEDs imaging method would then provide highly desirable information with regard to the underlying seizure source network, which would help to define the SOZ.

To better capture the dynamics of inter-ictal activities, the imaging techniques with high temporal resolution are required to separate the primary seizure focus from propagation areas. It is important to note that IEDs may also have rich spatiotemporal dynamics, which can be studied in order to better delineate the origins of the epileptic activity. In this context, the high temporal resolution of scalp electro-encephalography (EEG) and magneto-encephalography (MEG) allows the detection of the fast propagating IEDs more efficiently than other non-invasive imaging techniques (Brookes et al. 2014; J. S. Ebersole and Ebersole 2010), as shown in Figure 1 (Bin He et al. 2011).

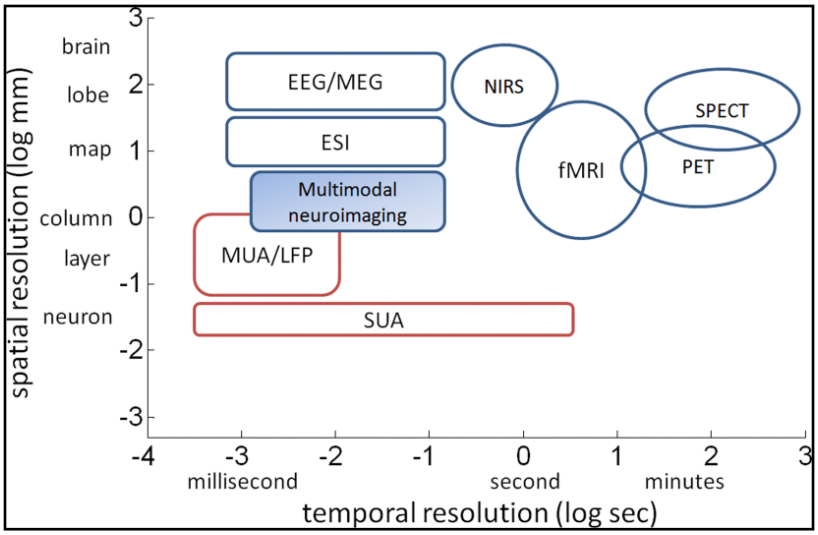

Figure 1. Schematic illustration of the ranges of spatial and temporal resolution of various noninvasive (in blue) imaging techniques and invasive (in red) experimental techniques. Among the neural recording technologies listed, the intracranial recordings single-unit activity (SUA), multi-unit activity (MUA), local field potential (LFP) have higher spatial/temporal resolution, specificity but limited coverage. While the other imaging modalities based on hemodynamic measurements, such as the functional magnetic resonance imaging (fMRI), provide high spatial resolution in imaging brain activity but are limited in their low temporal resolution and interpretation in terms of the underlying neuronal activities.

However, both MEG and EEG face the problem that the signals measured on the scalp surface do not directly indicate the location of the active neurons in the brain, which leads to their limited spatial resolution (Helmholtz 1853; FENDER 1987). In this context, applying source imaging technique based on solving the inverse problem has been explored to show reasonable accuracy (Ding et al. 2006; Ding et al. 2007; Grova et al. 2006; Krings et al. 1998; Lu et al. 2012; Michel et al. 2004). MEG/EEG inverse problem is established based on the principles of bio-electromagnetism. Due to the ambiguity of such a problem, i.e. a given electric potential or magnetic field recorded at the scalp can be explained by the activity of infinite different configurations of intracranial sources (Helmholtz 1853), it can only be solved by introducing a priori assumptions on the generation of EEG and MEG signals (FENDER 1987). The more appropriate these assumptions are, the more trustable are the source estimations. During the last two decades, different assumptions have been formulated, and implemented into different models

as depicted in (Brookes et al. 2014; Baillet and Garnero 1997; Huang et al. 2007; de Peralta Menendez and Gonzalez-Andino 1998; Hämäläinen et al. 1993; Ding and He 2004).

Generally, there are two main kind of models for solving inverse problem (Ding and He 2004). One is dipolar (overdetermined) model, where the basic a priori assumption is that only a small number of current sources in the brain can adequately model the surface measurements. To ensure a unique solution, the number of unknown parameters has to be less than or equal to the number of independent measurements (i.e. electrodes). The second model is the distributed source (underdetermined) model, which is based on reconstruction of the brain electric activity in each point of a 3D grid of solution points, where the number of points being much larger than the number of measurements. Thus, there would be no a priori assumption about the number of dipoles, as each solution point will be considered as a possible current source.

Both models have advantages and disadvantages comparing to the other. The major difficulties faced by overdetermined model is to determine the number of dipoles (Ding and He 2004). Most often, the choice could be based on physiological knowledge of how neural activity is generated. However, this could be a risky assumption given the fast propagation of brain responses and parallel activation of primary and secondary sensory areas (Said 2001; Blanke et al. 1999), especially the inter-ictal activities in epilepsy (Huppertz et al. 2001). On the other hand, the major disadvantage of underdetermined model is the huge number of unknowns (more than 10,000), which means within the 3D grid of solution points, an infinite number of distributions of current sources can lead to the same scalp potential map. A regularization need be added to solve such a problem. The regularization term is usually based on a priori assumption, for example, the Minimum Norm (MN) solution which assumes that the 3D current distribution should have minimum overall intensity (smallest L2-norm) (Hämäläinen and Ilmoniemi 1994) . Both models have been applied to localize brain activities successfully.

With high temporal resolution of MEG/EEG and source imaging technique, a classical approach for the IEDs localization process would include detecting IEDs, averaging IEDs, peak selection, followed by source localization on the peak to infer the brain generators of the observed signals. However, whatever is the process chosen to classify spikes, averaging might lead to some signal cancellation, which is more likely to filter out source activities that vary slightly over each individual spike (Ahlfors, Han, Lin, et al. 2010), especially when the time point selected to align the spikes for averaging is different for each spike. To this end, some researchers (Aydin et al. 2015) suggested to combine bootstrap techniques and sub-averaging to increase SNR while preserving some inter-spike variability, which has shown good result when the number of measurements is limited (Chowdhury et al. 2017). Moreover, inter-ictal activities are usually observed as a train of peaks in multiple regions with latency, suggesting that spikes can propagate very rapidly across the cortex. By mapping spike propagation through the cortex, several studies have correlated propagation with important clinical variables such as epileptic pathology and SOZ localization (Baumgartner et al. 1995; Hara et al. 2007).

In a word, accurate detection and localization of propagation pattern of individual inter-ictal spike will be essential to capture the dynamics of IEDs, thus leading to the detection of the underlying epileptic network. The MEG/EEG will be optimal non-invasive imaging technique due to its high temporal resolution as well as high spatial resolution improved by source imaging. **Therefore, in this thesis study, we propose that a spatiotemporal analysis can characterize the underlying generators of IEDs better than classic analysis method alone.** Following the detection and classification of inter-ictal spikes, we compared the source localization result from averaged spikes to the result after spatiotemporal analyses. Each individual IED was analyzed spatiotemporally to extract most information, in order to then reconstruct the epileptic network. Connectivity analysis was used to assess correlations revealed by spatiotemporal analysis.

Simulation

Source Imaging Simulation:

Monte Carlo simulation was conducted to test the accuracy of MEG/EEG source imaging technique and the impact of high-density MEG/EEG recording comparing to low-density.

Forward Model:

To solve the inverse problem, correlation between brain cortex and surface measurements (EEG/MEG) needs to be built, which is the so-called forward problem. Different models were constructed based on the physical properties of the brain, including two main categories: simple head model which assume the head to be in a spherical shape, and realistic head model which is based on MRI image. A detailed discussion could be found in (Wendel et al. 2009; Hallez et al. 2007). In this simulation, a realistic head model based on Boundary Element Method (BEM) (He et al. 1987) was applied. A high resolution T1-weighted anatomical MRI of a healthy subject was used to segment the surfaces of the brain to obtain the realistic head model.

The correct modeling of head tissue conductivities, especially the conductivity ratio of the skull relative to brain and scalp is an important parameter that determines the accuracy of the forward and inverse solution especially in EEG. From past studies, (Oostendorp and Delbeke 1999; Malmivuo and Suihko 2001; Lai et al. 2005; Zhang, van Drongelen, Bin He 2006; Huiskamp 2008; Vallaghé and Clerc 2009; Chen, Hallez, and Staelens 2010), brain-to-skull conductivity ratio between 1:20 was found most acceptable for the adult brain. Using the software Curry 8 (Compumedics, Chalotte, NC), a 3-layer EEG BEM model consisting of the inner skull, outer skull and the scalp (conductivity values of 0.33:0.0165:0.33 S/m) and a 1-layer MEG BEM model consisting of the inner skull (conductivity value of 0.33 S/m) were generated.

Inverse Problem

The cortical current density (CCD) source model (one of the distributed source models) (Dale and Sereno 1993) were used in the present study, in which the source space will be represented numerically by continuously distributed triangular elements over the cortical surface. Each triangular element models the source on itself by a current dipole oriented perpendicular to the local surface. The brain electrical activity can be modeled by current dipole distributions where a large number of dipolar sources are distributed along the cortical surface. The relation between the current dipole distribution and the scalp EEG/MEG is constituted by Maxwell's equations. The CCD model was obtained by segmenting the white matter/gray matter interface from the human head MRI (the same one as in forward model) using the Curry software. After discretizing the solution space and numerically solving Maxwell's equations, a linear relationship between the current dipole distribution and the scalp EEG/ MEG can be derived as:

$$\vec{\varphi}_{M/EEG} = \mathrm{K}_{M/EEG}\vec{\mathrm{J}} + \vec{\mathrm{n}}_{M/EEG}$$

where vector J represents elemental dipole moments defined on the CCD model, and vector φ is the electrical potentials and magnetic fields measured, K is the lead field matrix calculated by using BEM model constructed in the forward problem. The n denotes background and measurement noise in EEG and MEG.

In this simulation, one commonly used inverse algorithm, the standardized low-resolution electromagnetic tomography (sLORETA) (Pascual-Marqui 2002), was applied to obtain the underlying neuronal activity. The algorithm is based on MN estimates, but further divides the MN solution by the estimated source covariance at each dipole location to accommodate for the distortion and noise variation. Thus, the sLORETA is widely accepted to give an unbiased accurate solution. The input would be the measurements from different modalities and BEM

model constructed from structural MRI, and the output would be the F-statistics of current density in the cortex surface model. Larger value shows stronger activation.

Impact of Model-Error

The use of same head model during forward and inverse problem can lead to the best case in any simulation study. A thorough discussion about the so-called inverse crime could be found in (Sohrabpour, Lu, et al. 2016). In order to mimic the real data scenario, we can introduce noise in the measurements through different model for inverse and forward in simulations (G. Wang and Ren 2013). In this simulation, finer grid size of cortical segmentation (2 mm) was applied in forward model to construct more accurate measurements, while the grid size used for inverse problem solving was coarse (2.5 mm).

Simulation Protocol

The single source model was considered, and the locations of the dipole source were generated randomly on a realistic cortex segmented from a human MRI template (very deep nodes near the thalamus or in the inter-hemisphere region were excluded). Orientations of sources were perpendicular to the cortex surface. The time activity of the source was simulated based on a realistic inter-ictal spike time course from an epilepsy patient.

Different configurations of MEG and EEG were considered in this simulation. EEG electrode locations and MEG sensor locations and orientations were adopted from the realistic EEG and MEG systems. In order to simulate similar spatial coverage of EEG sensors as that of MEG, a subset of 120 EEG channels was selected from a realistic 128-electrode EGI system (Electrical Geodesics, Inc., Eugene, OR) by removing some electrodes on the face. EEG channels

were then evenly down-sampled in space to 60 and 30 locations to simulate different numbers of electrodes covering similar area of sampling space. For MEG, there were 148 MEG sensors from a 4Dneuroimaging MEG system, and the down-sampled configuration of 74 and 37 channels were generated.

EEG and MEG data were constructed by applying the corresponding forward model with different measurements to the simulated current density with randomly selected dipole location respectively. Both Gaussian white noise and realistic physiological noise extracted from a 3 min segment of EEG/MEG background activity acquired on healthy subjects were added to the simulated data. The amplitude of the background activity trials will be scaled to ensure an average signal-to-noise (SNR) ratio of 5, 10, 20 dB separately to evaluate the sensitivity to noise level. After that, the inverse problem was solved to obtain activation time course for each source location. The localization result were considered as the source activation at the maximum of global field potential (GFP). For each condition, the whole process was repeated for 100 times.

Evaluation Metrics

The localization results were evaluated by localization error (LE) which is calculated as the Euclidean distance from simulated source to the maximum of the localization result. The smaller LE is, the more accurate source localization is.

Result & Discussion

The localization error (in mm) is shown as Figure 2.

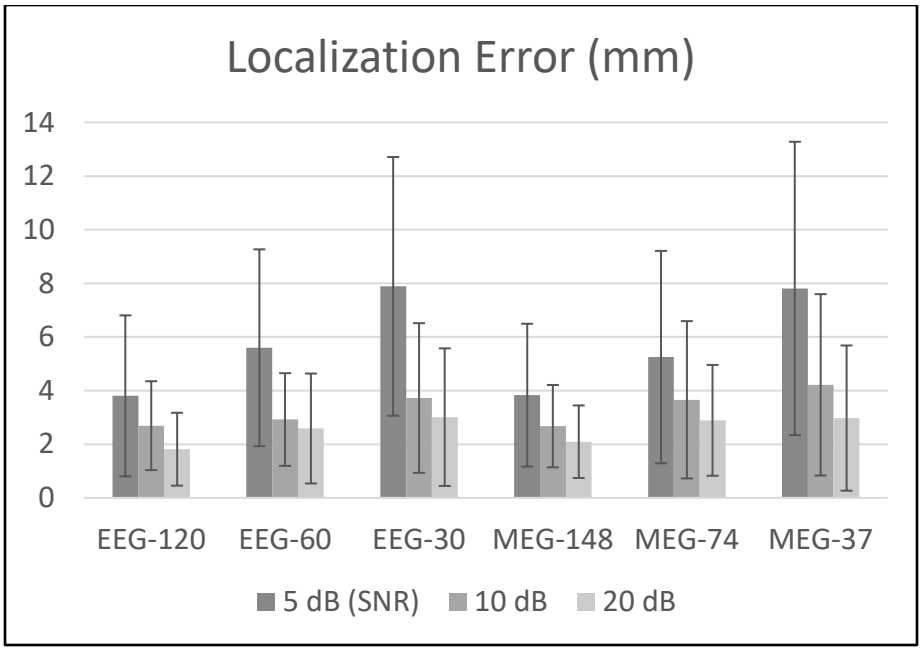

Figure 2. The average localization error simulated. EEG with 120, 60, 30 channels are simulated, MEG with 148, 74, 30 channels are simulated. Different levels of noise (5, 10, 20 dB Signal-to-Noise Ratio) were added to the constructed signal to mimic realistic situation. The dark lines show the standard deviation.

The simulation results show that increased measurement number (electrodes, sensors) decreased the localization error significantly. MEG and EEG localization accuracy is very similar. In a simulation with 10 dB noise or better and 60 or more measurements, the average source localization error could be as small as about 5mm.

The simulation verifies the accuracy of source imaging technique when applied to MEG or EEG, which is the foundation of the following analysis on clinical data.

Topo Map Extraction Simulation:

Monte Carlo simulation was conducted to compare the classical spike averaging method with spatiotemporal method regarding extracting activation topographic maps (topo maps), which is the visual-spatial illustration of brain activation (Nuwer 1988).

Simulation Protocol

The same forward model and cortex segmentation as in previous session (Source Imaging Simulation) were adopted in this simulation. Two-source model was considered. The locations of the dipole source were generated randomly and the orientations of sources were perpendicular to the cortex surface. The time activity of the source was simulated as a spike using a Gaussian pulse, as shown in the right panel of Figure 3a).

To mimic a realistic situation where a weak peak leading the main peak in a train of spikes, the amplitude of the first source was simulated as 5 times larger than the second one, while the activation peak of the first source is behind the second source by around 50 ms, as shown in Figure 3. The time lag between the two sources were jittered. 148-channel MEG configuration was used. MEG data were constructed by applying the forward model to the simulated current density with randomly selected dipole locations respectively. 10 dB background noise was added to the simulated measurements.

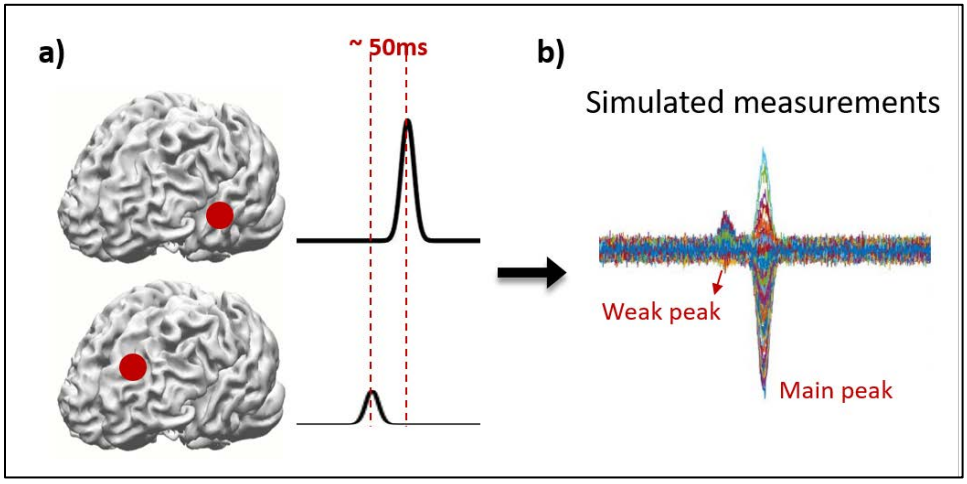

Figure 3. a) The simulation protocol. To mimic a realistic situation where a weak peak leading the main peak in a train of spikes, the amplitude of time course for the first one was simulated as 5 times larger than the second one, while the activation peak of the first source is behind the second source by around 50 ms. b) simulated measurements.

For each source location configuration, 10 spikes were constructed. Each spike was slightly different from others due to jittered time lag and background noise.

Two methods for extracting topo maps were applied to the simulated measurements. For the spike averaging method, each set of spikes was averaged over the peak of time course, and the main peak and weak peak were defined as the two local maximums of the GFP. Topo maps were then extracted on the two peaks found. For the spatiotemporal analysis method, each set of spikes were concatenated together, and Independent Component Analysis (ICA) (Hyvärinen, Karhunen, and Oja 2004) was then applied to the concatenated signal. The two main components which showed significant activation were then defined as the extracted topo maps.

The whole process was repeated for 100 times.

Evaluation Metrics

For each source, the standard topo maps were calculated using the same forward model and no noise was added. Topo maps from spike averaging method and spatiotemporal analysis were compared to the standard maps.

The topo map similarity was defined as the correlation of standard maps with the extracted maps from each method. The maximum of correlation is 1. The closer the correlation to 1, the more accurate the map is.

Result & Discussion

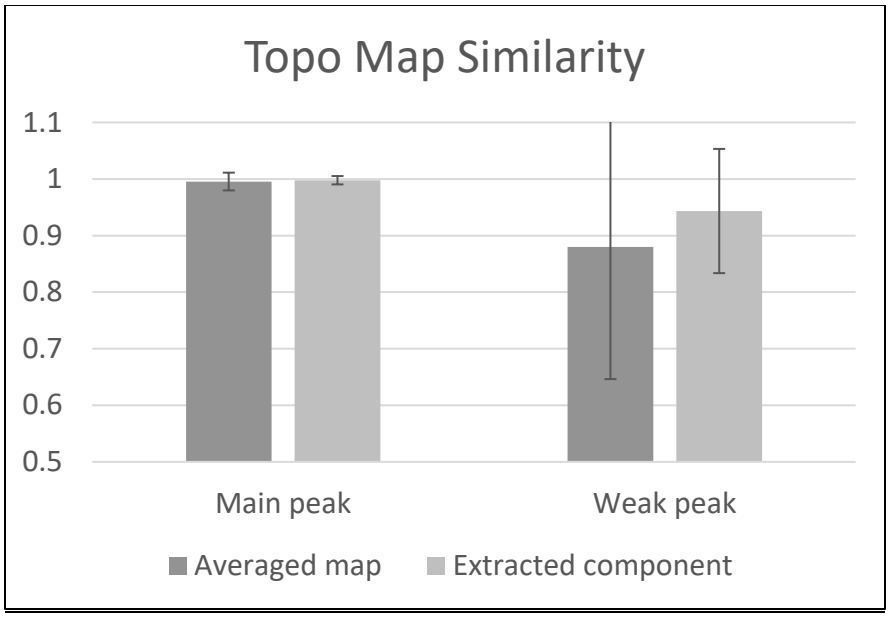

Figure 4. The topo map similarity comparison. No significant difference is shown for the topo maps of the main peak. For the weak peak, the spatiotemporal analysis shows higher and more stable correlation according to the mean and standard deviation of the correlation in 100 trials.

The simulation results show that even though there is no significant difference between the two methods regarding the extracting the main peak, spatiotemporal analysis performs better in extracting the weak peak. The averaged correlation is higher, and the standard deviation among 100 trials is much smaller as well.

The simulation suggests that when there is a spike propagation process, especially when the secondary activation is stronger than the first activation, spatiotemporal analysis on individual spikes may give a better result regarding extracting the topo maps for further analysis.

Data Acquisition

After evaluating the source imaging technique and the possible improvement of extracting topo maps by adding spatiotemporal analysis to individual spikes, EEG/MEG recordings from epilepsy patients were obtained for further validation. Four patients with medically intractable epilepsy were studied using a protocol approved by the Institutional Review Boards of the University of Minnesota and Allina Hospitals and Clinics. The patients were selected according to the following criteria: (1) anatomical MRIs and inter-ictal MEG/EEGs were recorded preoperatively; (2) the patients underwent resection of epileptogenic zones identified clinically; (3) the patients had at least 1 year follow-up after the surgical resection. The epileptogenic foci in the patients were identified by experienced epileptologists according to ictal onset zones localized using intracranial EEGs.

Three of the patients were seizure-free or had significant seizure reduction with AEDs (anti-epileptic drugs) after surgical resection. The other one is not seizure-free after surgical resection. The clinical information of the four patients with medically intractable epilepsy is summarized in Table 1.

Table 1. Patient Information

Patient	EEG	MEG	Resection	Follow-up
1	64-channel	148-channel	Left temporal	Seizure-free
2	NA	148-channel	Left temporal	Not seizure-free
3	NA	148-channel	Left temporal	Seizure-free
4	NA	148-channel	Left temporal	Seizure-free

The inter-ictal MEG data was recorded by Magnes 2500 WH (148 MEG channels, 4D Neuroimaging). The patients lay in a magnetically shielded room without motion during MEG recording. One patient underwent simultaneous MEG/EEG recording. For patients with MEG only, the inter-ictal MEG data were sampled at 508.63 Hz and continuously acquired with an online 1 Hz high-pass filter. For simultaneous MEG/EEG recording, inter-ictal MEG/EEG data were sampled at 1Hz and continuously acquired with an online 1 Hz high-pass filter. The anatomical MRIs for source imaging include a three dimensional T1 weighted sequence, acquired on a 1.5T or 3T GE scanner. The inter-ictal MEG/EEG data were filtered with a 30 Hz low-pass filter (zero-phase filtering) to remove high frequency artifacts but preserve frequency components up to the beta band. Corrupted channels were rejected by visual inspection.

Methods

Classical Analysis Protocol

For each patient, significant inter-ictal spikes were selected and reviewed by experienced epileptologists. The spike sets for each patient were selected manually without any a priori information. Each spike is a segment of 1 second encompassing the spike peak. Each spike set was then averaged over the peak. After that, the spikes were classified according to morphology, state transitions and topographic maps. The classification of spikes was also reviewed and confirmed by epileptologists. The peak of spike was defined as the first significant local maximum of global field power.

The classical spike analysis method was firstly applied, the framework of which is shown in Figure 5. Each sets of spikes were averaged over the peak to increase the SNR. Source imaging

techniques were then applied on the averaged spike on the primary peak to find the region of interest (ROI). The anatomical MRIs of patients were used to segment the surfaces of the brain to obtain the realistic head model. sLORETA algorithm was used to solve the inverse problem. A detailed discussion about source imaging could be found in Simulation section.

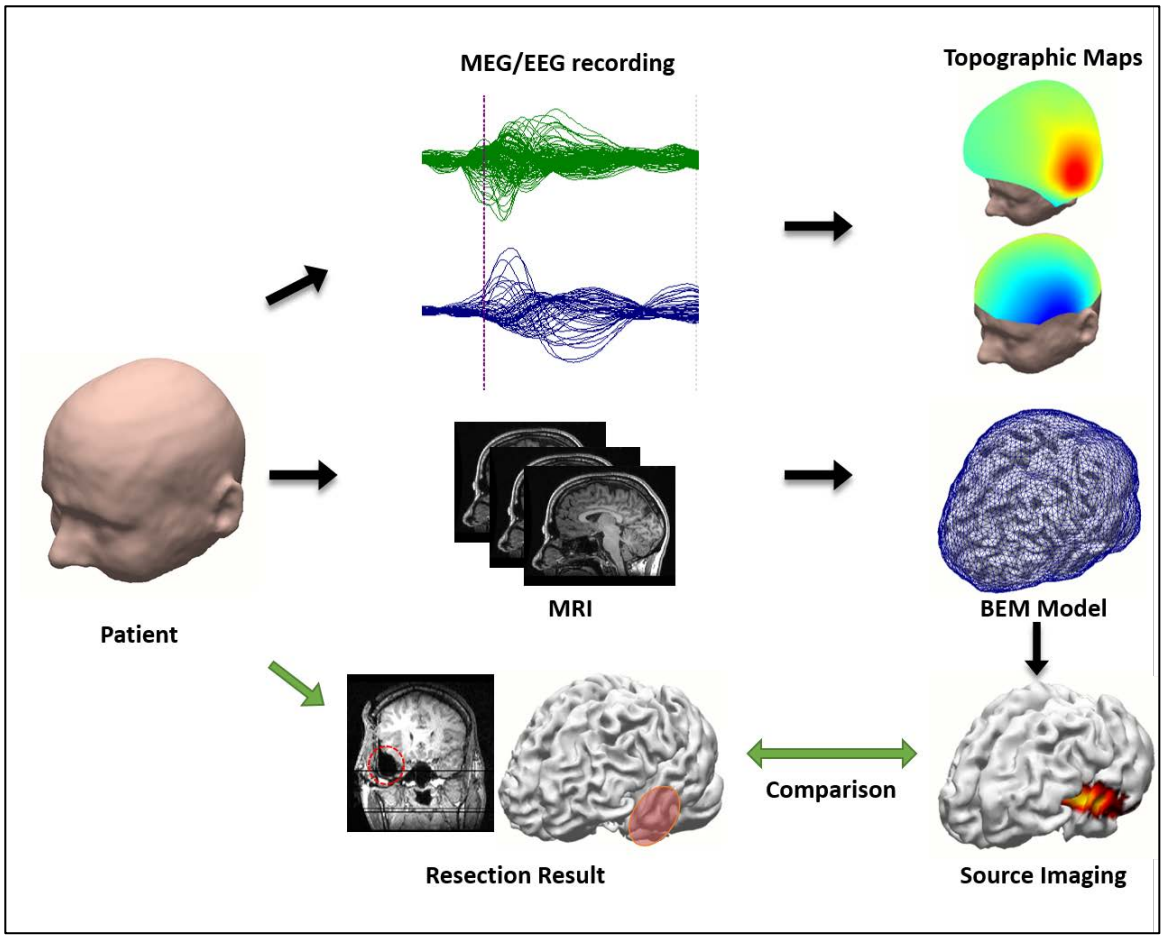

Figure 5. Illustration diagram of classical EEG/MEG spike analysis method. Topo maps extracted from EEG/MEG and BEM model constructed from MRI are used to solve the inverse problem. The source imaging results are compared with clinical resection result from post-operational MRI to evaluate the accuracy of the method.

Spatiotemporal Analysis Protocol

To better extract the sequential activation and ensure the accuracy of averaging result, spatiotemporal analysis was added into the classical protocol. After the averaged spike study, all

the spikes in each spike set were concatenated. ICA was then applied on the concatenated data to separates the scalp MEG/EEG into independent components (ICs) in sensor space. In the analysis, the MEG/EEG was decomposed into temporally independent and spatially fixed components. The components characterized by temporal-spectral patterns of inter-ictal activity were selected, based on the consistency of component activation time among all spikes and the averaged activation time course.

The earliest component found in the selected components was compared with the topo map extracted from the averaged spike. If any inconsistency found, the connectivity analysis was then applied to verify the results. The results from averaged spike analysis, spatiotemporal analysis, and connectivity analysis were integrated together, and then compared with surgical resection to evaluate the method.

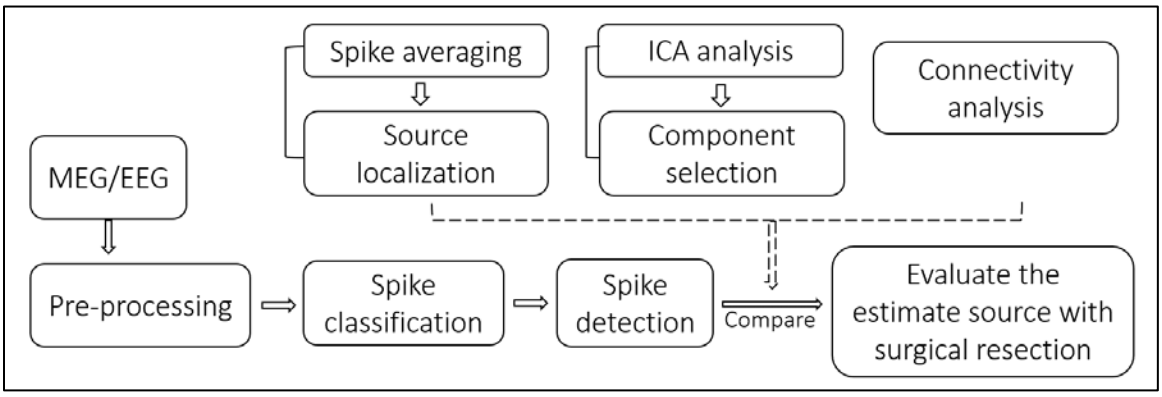

Figure 6. Spike analysis protocol with spatiotemporal analysis and connectivity analysis added.

Component Selection

Components that correspond to artifacts, such as eye blinks and motion artifacts, were removed from the decomposed ICs (Jung et al., 2000). The spectrogram of each IC was calculated using a short-time Fourier transform with the time window of 100 samples and 50%

overlapping to show. The activation time courses were calculated for each IC to show their temporal correlation.

Two metrics were used to select ICs significant activated among all spikes. The correlations of spectrograms among each spike set were calculated to measure if the IC is activated in the majority of spikes in the same set. The activation time courses for each IC in all spikes were averaged, and the averaged time courses before spike onset (500 ms before the main peak) and after the spike onset were compared. The IC was rejected if no significant difference found.

Connectivity Analysis

In the patient's data where inconsistency was found between the averaged spike and spatiotemporal analysis, connectivity analysis (Sohrabpour, Ye, et al. 2016) was conducted to explore the correlation between the possible seizure onset zones (SOZs). Utilizing the theory of Granger causality (Granger and Granger 2001) and computing adaptive directed transfer function (ADTF), which provides a spectral measure for directed connections among the modeled time series, directional connectivity among the ROIs (determined by source imaging) was estimated from the activity time-course (estimated from source-imaging results). The multivariate autoregressive (MVAR) model was first fit to the time series as

$$\mathrm{X(t)} = \sum_{i=1}^{p} A(i)X(t-i) + \varepsilon(t)$$

Where $X(t)$ is the multidimensional time series under study, $A(i)$ are coefficient matrices of the MVAR model to be estimated, and $\varepsilon(t)$ is the vector of white noise, driving the MVAR model. The order of this MVAR model is p, as the model leans upon the effect of p previous

values of the time series to predict the future values. The transfer function of the system could be derived by taking the Fourier transform of the equation and inverting the coefficient matrix as:

$$\mathrm{A(f)X(f)} = E(f) \rightarrow X(f) = A(f)^{-1}E(f) = H(f)E(f)$$

where $H(f)$ is the transfer matrix of the system. The Direct Transfer Function (DTF) value $\gamma_{ij}(f)$ represents the signal flow from time series of node j to node i, which can be obtained as follows:

$$\gamma_{ij}(f) = \frac{\left|H_{ij}(f)\right|^2}{\sum_{m=1}^{n}\left|H_{ij}(f)\right|^2}$$

As the relationship between the ADTF and the time series are highly nonlinear, a nonparametric statistical testing was employed to reject spurious connections due to random noise. The surrogate data was generated by keeping the amplitude of the time-series spectrum the same as the original data but permuting the phases. This shuffling procedure was performed 1000 times and if the ADTF value computed passed the significance level ($p < 0.05$), they were kept, otherwise replaced by zero. This shuffling process was performed for all ADTF analysis.

Results

Patient 1

Figure 7 shows averaged spike source imaging result for Patient 1 who had left temporal seizures as well as left parietal lesion identified from structural MRI by clinicians. Two sets of spikes (both observed in EEG and MEG) were observed by looking at their morphology and state transition, and the inverse problem was solved for the peak of the averaged spikes to find the region of interest (ROI). One set of the extracted spikes (21 spikes in EEG and 23 spikes in MEG)

was localized to the temporal region, and the other set (8 spikes in EEG and 8 spikes in MEG) to the left parietal–occipital region. ROIs found using both EEG spikes and MEG spikes overlap well with each other (ROI centers are within 10 mm). In Figure 7, the source locations and extent (80% threshold) are displayed with the cortex model constructed from the preoperative MRI of the patient. The averaged spikes are also displayed next to the sources in Figure 7. Spikes in the left column (spike 1) were used to find ROI 1 and spikes in the right column (spike 2) were used to find ROI 2.

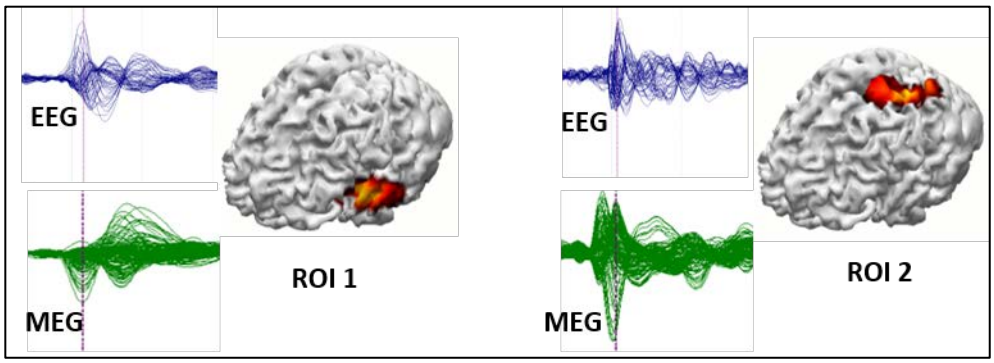

Figure 7. Averaged inter-ictal spikes and estimated sources (80% threshold). © 2016, IEEE

To explore the correlation between the two spike sets and two ROIs, spatiotemporal analysis was conducted on both spike sets. All spikes in each spike set were concatenated together and then filtered between 1 to 30 Hz. Figure 8 shows the spatiotemporal analysis results of this patient for two spike sets. Multiple components were extracted and the significant components were selected. Significant components selected were arranged in order of activation timing (first peak in averaged activation time course).

The main component in each spike set which shows the best consistency among all spikes represents the peak activities very well (Component 1 showing left temporal activation on in

spike set 1, Component 2 showing left parietal activation in spike set 2). However, the components showing the earliest activation is very similar in two spike sets as shown in Figure 8. The scalp map suggests left temporal focus of the activity. Note that in spike set 2, the earliest component is very weak, and the timing is not consistent among all spikes, which may be the reason of cancellation in spike averaging.

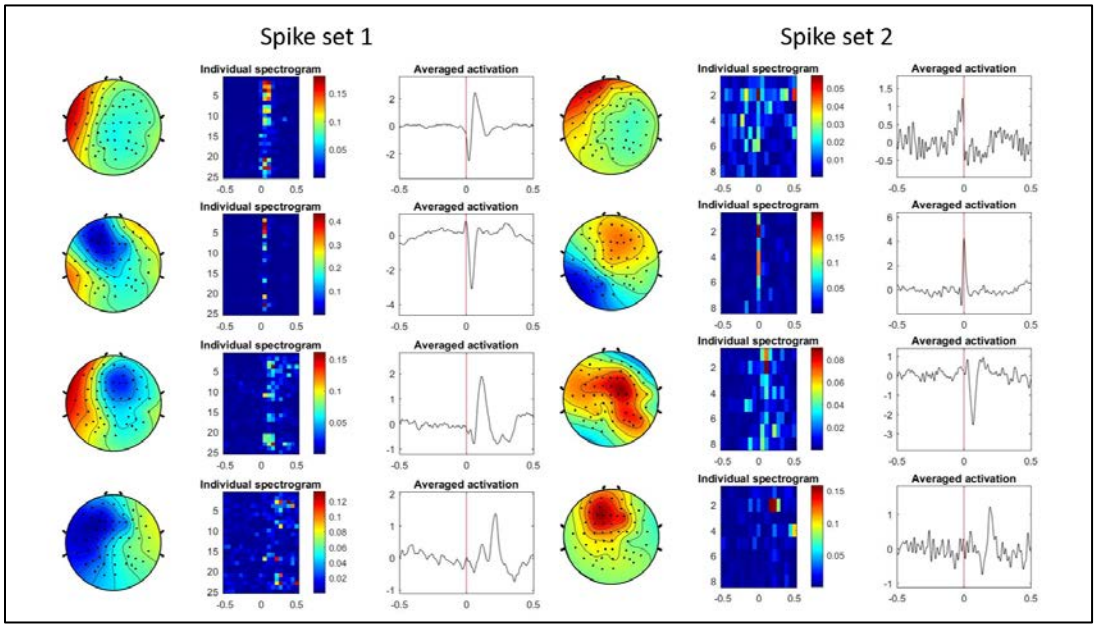

Figure 8. The result of spatiotemporal analysis in Patient 1. The left panel shows significant components in spike set 1. The right panel shows significant components in spike set 2. For each component, 3 figures showing different features are presented. Topo map is shown in the left side. The integrated spectrogram for all the individual spikes in the middle. Each row in the spectrogram represents the activation pattern in one individual spike. The right figure is the average of all the activation time course among all the spikes in one spike set. The red line indicates the peak of averaged Global Field Power where the source imaging was applied in Figure 7.

Further connectivity analysis results confirmed the findings from spatiotemporal spike analysis. The significance level of DTF information flow between ROI 1 and ROI 2 is depicted in Figure 9(a) as a function of frequency. What these curves reflect is the significance of the calculated DTF value as compared to the surrogate DTF values for every frequency in the 1–15 Hz frequency band where signal power is most concentrated in; thus, only DTF values that are

statistically significant and are above the red line indicate meaningful connections. DTF results above the red line pass the significance level ($p<0.05$) of the information flow and are thus significant. In this patient, ROI 1 shows significant information flow to ROI 2 while no such significance can be observed from ROI 2 to ROI 1. Both spike 1 and spike 2 were used to calculate the DTF values. The connectivity results presented in Figure 9(a) indicate that the flow from ROI 1 to ROI 2 passes the significance level (left column) while the flow from ROI 2 to ROI 1 does not pass the significance level (right column). This can be also seen from the information flow direction (from temporal ROI to parietal ROI) and the comparison of total outflow volume (temporal ROI significantly larger than parietal ROI) in Figure 9(b).

Thus, ROI 1 located in the left temporal lobe was identified as the primary source. Figure 9(c) shows the postoperative MR image with the red line marking out the surgically resected area. The resection is also approximately marked with the red oval on the cortex. The results indicate that source-imaging results and connectivity analysis results from EEG/MEG coincide well with the clinical findings and analyzing IEDs network helped to on the underlying epileptic network. **The patient is seizure-free after the resection.**

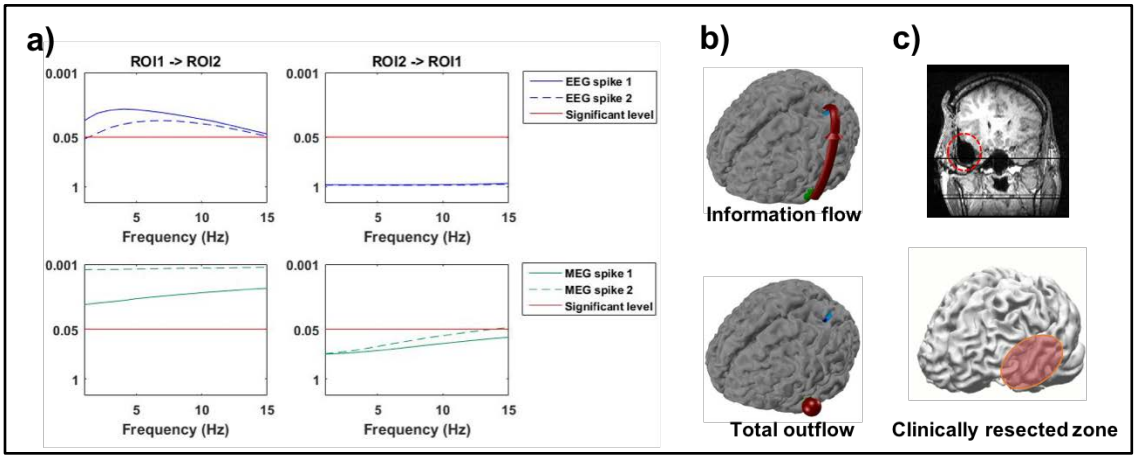

Figure 9. Identifying epileptic networks from IEDs in Patient 1. (a) Statistical testing results of DTF values between the two ROIs. DTF values above the red line are significant with a corresponding p-value < 0.05. (b) Information flow

direction and comparison of total outflow volumes between the two ROIs depicted on cortex model. (c) Surgical resection marked by red dotted line on post-operative MR image and red oval on the cortex model. This patient suffered from left temporal lobe epilepsy before surgery. After the resection, the patient is seizure-free. © 2016, IEEE

Patient 2

Figure 10 shows averaged spike source imaging result for Patient 2. One spike set containing 10 spikes was found in this patient in MEG. The spikes were averaged and the sLORETA solution was obtained to find ROIs. The extracted spikes localized to the frontal-parietal region where the inverse problem was solved for the peak of the averaged spike.

Two earliest significant components were found to show overlap around the spike peak. One is significant in a subset of spikes, the other one is significant among all spikes (shown in Figure 10). By solving inverse problem on topo map of each component, Component 1 was found to be localized more towards left frontal lobe while Component 2 was found to be localized more towards left parietal lobe. From the averaged activation time course, the first peak in parietal lobe activation is earlier, which may suggest a left parietal onset zone.

These two components overlapped spatially, which resulted in the frontal-temporal source found when solving inverse problem in the averaged peak. By looking at the spectrogram of individual spikes and the activation time course, the two components could be spatiotemporally separated. This result may suggest a transient propagation from parietal region to frontal region. **The patient is not seizure-free after left temporal lobectomy, which supports the possibility of a different seizure onset zone.**

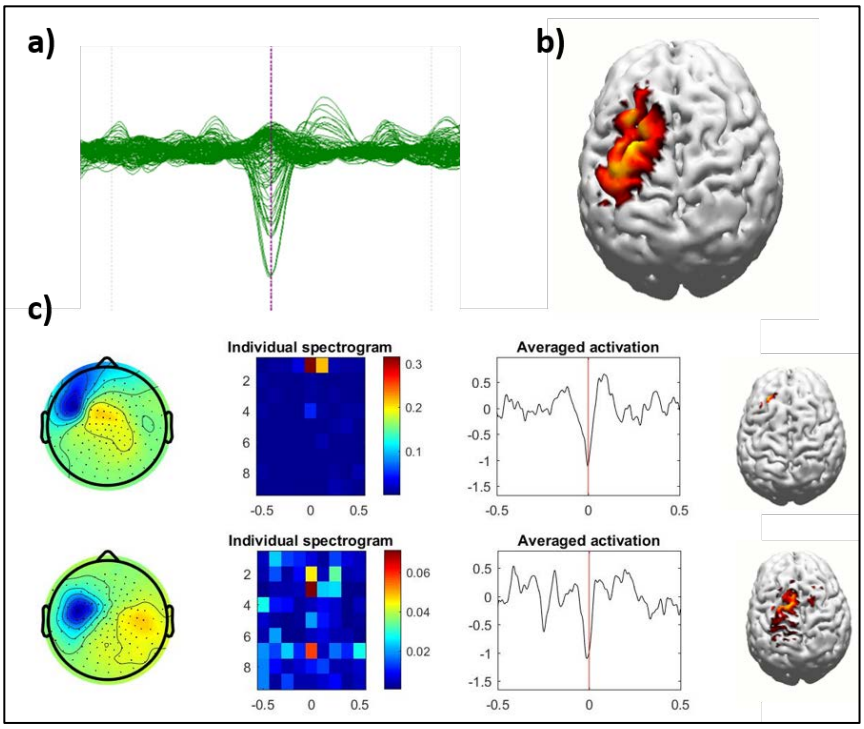

Figure 10. Analysis result for Patient 2. a) Averaged spike in MEG. b) Source localization result at the peak of averaged spike (marked with red line in a). c) Spatiotemporal analysis result. Note that the first component (upper one) is stronger and more towards frontal lobe. The second component is more consistent among all spikes but more towards parietal lobe. The patient is not seizure-free.

Patient 3 and Patient 4

Figure 11 shows averaged spike source imaging result for Patient 3 and Patient 4 who had left temporal seizures and received lobectomy. In Patient 3, one spike set containing 15 spikes was found showing source localization in the left temporal lobe. In Patient 4, one spike set containing 15 spikes was found showing source localization in the left temporal lobe as well. The earliest significant component from spatiotemporal analysis was shown, which coincided well with the peak in averaged spike. **Both patients underwent temporal lobe resection and they are seizure-free now.**

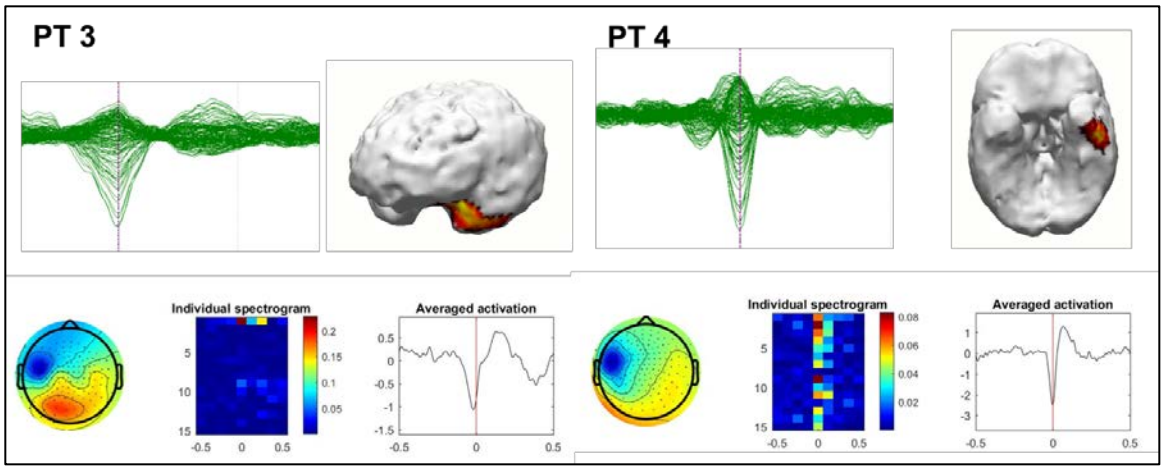

Figure 11. Analysis result for Patient 3 and Patient 4. Averaged spike for both patients shows temporal source when applying inverse problem on the peak of averaged spike. The earliest significant components shown at the bottom row also confirm that only one major component is activated at the peak, which indicated a focal activation Source found in both patients coincide well with resection. Both patients are seizure-free.

Discussion

In this study, we examined an analysis pipeline of inter-ictal MEG/EEG for estimating the most likely primary epileptic sources and the propagations activities in 4 medically intractable epilepsy patients. The analysis method mainly included three steps: cortical source imaging from MEG/EEG, spatiotemporal analysis to get propagation topo maps, and cortical ROI connectivity analysis. The distributed source model with the three-layer BEM was used for cortical source imaging, and the DTF was employed for the calculation of directional connectivity among multiple cortical ROIs.

Spatiotemporal Analysis of Individual Spike

In 2 out of 4 patients analyzed, inconsistency was found between averaged spike result and spatiotemporal analysis. 1 patient with consistent spatiotemporal analysis result and connectivity result was seizure-free. 2 patients with consistent spatiotemporal analysis result and averaged spike analysis were seizure-free. The present results suggest that the sources estimated from the inter-ictal spikes in each patient partially agreed with the epileptogenic zones identified clinically. The estimated propagations of the epileptic activities, which were shown to be related to the outcome of epilepsy surgery in this study, might represent epileptic networks.

Spike averaging has been adopted in most studies (Bast et al. 2004; Dai et al. 2012; Hara et al. 2007; Chowdhury et al. 2013; Sohrabpour, Lu, et al. 2016; Ding et al. 2006) to increase the SNR and improve the reliability of the source localization solutions. However, it is well known that waveforms of individual spikes might actually be quite variable in epileptic patients (Köhling et al. 2000). Therefore, averaging effect is very likely to filter out source activities, which could slightly vary over each individual spike. According to standard averaged spike localizations results shown in this study, we noticed that even though averaging did increase the SNR,

sometimes the true sources were diminished, thus resulted in localization errors.

This shows that source imaging on averaged spike combined with spatiotemporal map estimate might create a balance between spike variability and SNR. The extracted component topo maps could serve as a promising way of overcoming the limitations of averaged spike localizations and extracting the most reliable and reproducible source among the single spike sources. It is also important to emphasize that we were able to find at least one component that was fully concordant with the peak of averaged spike, as well as at least one component that was consistent among almost all individual spikes, which helped with successful localization in 3 cases. Moreover, in one case (Patient 2), the source imaging result is approximately between the two significant components we found, which suggesting that the averaged peak might be an overlapping of two components due to spike averaging. The patient is not seizure-free after left temporal resection, suggesting the parietal component (earlier one) to be the true source.

In a typical inter-ictal spike study, we only evaluated source localization results at the peak of the spike. However, the spatiotemporal analysis provides a series of topo map with activation time course, which is well-suited for the study of propagation patterns or other complicated epileptic patterns. The propagation patterns of inter-ictal spikes might potentially help with reconstructing the epileptic network if intracranial EEG available, which would enhance current understanding of mechanism of how inter-ictal spikes were generated.

MEG/EEG Source Imaging

In this study, 3 patients underwent MEG recording only, 1 patient underwent simultaneous MEG/EEG recording. Although the sources that produce EEG and MEG recordings are the same, i.e. synchronized postsynaptic currents in and around apical dendrites of pyramidal cells over an area of at least 1 cm^2 are the most easily detectable sources (Hämäläinen et al. 1993),

the distinct properties of the magnetic and electric field make the recorded signals different. From source location and orientation aspect, EEG is sensitive to both tangential and radial source while MEG is selectively sensitive to tangential sources(Neil Cuffin and Cohen 1979; Cohen and Cuffin 1987; Leahy et al. 1998; Huizenga et al. 2001; Gonçalves et al. 2003). This is caused by the sphere-like geometry of the head, which leads to strong canceling effect between magnetic fields produced by primary and volume currents (Cohen and Cuffin 1983; Hämäläinen et al. 1993). Moreover, sensitivity of MEG drops sharply as the depth of the source increases, while EEG degrades to a less degree than MEG (Hillebrand and Barnes 2002; Lin et al. 2006). However, from volume conduction aspect, accurate estimation of neuronal current with EEG depends on precise knowledge of the conductivity profile of the head tissues, particularly the skull which spatially smoothens and attenuates the electric potentials. On the contrary, the skull conductivity has almost negligible effects on magnetic fields recorded by the MEG (Hämäläinen and Sarvas 1989). Therefore, EEG is shown to be sensitive to uncertainty and variations in skull conductivities while MEG is largely insensitive to these changes.

Many studies have compared the performance of EEG and MEG in source localization. While some (Gharib et al. 1995) (Yamamoto et al. 1988) of them reported better source localization accuracy using MEG, others (Balish et al. 1991; Krings et al. 1998), however, indicated comparable performance of EEG and MEG. These conflicting data suggested various factors influencing the performance of EEG and MEG. As a result, the different sensitivity profiles and especially the complementarity of MEG and EEG encouraged researchers to increase the synergy by measuring and evaluating EEG and MEG simultaneously. Some clinical case reports and a blinded review study (Iwasaki et al. 2005; Knake et al. 2006) have addressed sensitivity variation, reporting different subsets of inter-ictal spikes which were visible commonly in EEG and MEG recordings or detectable in only one modality, suggesting an increased sensitivity of combining the two modalities together. From our pilot study in Patient 1, the

number of inter-ictal spikes found in MEG and EEG are different (23 in MEG, 21 in EEG, spike set 1), which is also a supporting evidence. The source imaging results of MEG and EEG both coincide well with the clinical findings. If more patients could be obtained with simultaneous MEG/EEG recording (preferably with comparable channel number), comparison could be made between the two imaging modalities in localizing IEDs in future study.

Moreover, several studies (Babiloni et al. 2001; Fuchs et al. 1998; A. K. Liu, Dale, and Belliveau 2002; Molins et al. 2008) have reported added accuracy of combining the complementarities of EEG and MEG data when performing source localization. Despite of the long history of MEG/EEG study and various attempts to compare their performance, to date, few studies have combined EEG and MEG data in recordings of real brain activities. Even among the few studies (Knake et al. 2006; Huizenga et al. 2001), MEG is usually in a favored position with more sensors than EEG electrodes. Also, lack of realistic head model constructed from individual MRI brought in extra errors into the already-imbalanced situation. In order to apply the novel technique to the study of IEDs in clinical settings, evaluation with simultaneous EEG/MEG recording from human subjects should be performed in future study.

While (Dai et al. 2012) used IEDs from MEG to study the epileptic networks and reported results which were in agreement with clinical findings, no study to date has applied the combined ESI and ADTF analysis in simultaneous EEG and MEG recordings to study epileptic networks, to the best of our knowledge. The combination could potentially provide more insight into the epileptic networks as EEG and MEG have different sensitivity to source location and orientation and thus could potentially provide complementary information about underlying epileptic sources (Ahlfors, Han, Belliveau, et al. 2010), (Goldenholz et al. 2009). The presented example in this study showed EEG and MEG results to be consistent and in agreement with each other, but combining them might lead to more comprehensive findings in the future. This could be also a direction for IED studies if more simultaneous MEG/EEG recording applicable.

High-density MEG/EEG Recording

In this study, we simulated the impact of electrodes/sensor number for MEG/EEG source imaging, the result of which match with literatures. In clinical studies, we used 148-channel MEG, which were shown to achieve an average localization error of less than 5 mm, as well as 64-channel EEG in one patient. The reason behind is, for inverse solutions to be accurate enough, the number of measurements needs to be large enough. Placing electrodes on the scalp can be thought of as a spatial sampling process (Tucker 1993); thus, using too few electrodes can result in under-sampling and aliasing happens. The effect of electrode numbers on source localization has been studied previously (Brodbeck et al. 2011), (Lu et al. 2012), (Sohrabpour et al. 2015), (Lantz et al. 2003).

As shown in these studies, source localization accuracy is improved when more electrodes are used but the rate of improvement decreases with the increasing electrode number. The optimal number of electrodes for MEG/EEG or combined MEG/EEG source imaging is still unclear, which may need further exploration in both simulation and clinical study.

Granger Causality

This study along with previous studies has shown the usefulness and strength of combining source imaging with directional functional connectivity analysis, in particular Granger–Geweke causality analysis (Astolfi et al. 2007), (Babiloni et al. 2005), (Dai et al. 2012), (Ding et al. 2007), (Lu et al. 2012), (He et al. 2011), (Sohrabpour, Ye, et al. 2016). Furthermore, we have shown in this study that source imaging algorithms could be used to identify network nodes in addition to activation time-course extraction, under realistic conditions and in data recorded in clinical settings.

Granger causality analysis is basically a data-driven technique, where no prior assumptions about the type, direction, and strength of interactions among the network nodes are assumed. The combined source imaging and A/DTF analysis presented in this study seems a viable path to objectively estimate network nodes and interactions. It has been tested in previous studies specifically in estimating epilepsy network nodes (Ding et al. 2007), (Lu et al. 2012),(Coben and Mohammad-Rezazadeh 2015).

In this thesis study, we looked at the application of Granger causality analysis in identifying epilepsy networks, as in such clinical cases independent information about the underlying sources and connectivity would be available through intracranial recordings or validated by surgical resection. Inter-ictal recordings from EEG and MEG (Dai et al. 2012) , as well as ictal signals have been analyzed to delineate underlying brain networks' connectivity (Ding et al. 2007), (Lu et al. 2012). Investigating network connectivity in resting state has also been adopted recently, and seems encouraging (Coito et al. 2016), (Elisevich et al. 2011). These functional connectivity studies add to our knowledge about localization and imaging of epileptogenic networks using various source-imaging techniques alone.

Overall, functional brain connectivity mapping could potentially help address the grand challenges of studying the brain. A number of studies have looked into various metrics of connectivity among multiple brain regions from EEG/MEG studies (He et al. 2011), (Ding et al. 2014), (Rocca et al. 2014), (Y. Liu, Moser, and Aviyente 2014) to fMRI studies (Jie et al. 2014), (A. Liu et al. 2014), (D. Wang et al. 2014). In addition to Granger causality, DCM approaches and graph theoretic methods have also been used to study brain functional connectivity from ECoG and EEG, which could be adapted in future study involving more complicated network.

Conclusion

In this thesis study, we developed a pipeline for inter-ictal spike analysis containing spike detection, classification, source imaging on averaged spike, spatiotemporal analysis of individual spikes for propagation pattern, as well as connectivity analysis for further confirmation. When compared with standard averaged spike source localization, the spatiotemporal analysis on individual spikes and the connectivity analysis provided the second step confirmation to ensure successful source localization in studied cases.

In conclusion, high-density MEG/EEG recording along with source imaging could be used as a valuable non-invasive tool during pre-surgical diagnosis of patients with epilepsy. While classical method for spike analysis might lead to multiple ROIs and thus inaccurate results, spatiotemporal analysis along with connectivity analysis could be helpful to identify the underlying epileptic network, therefore determine the seizure onset zone accordingly.

Bibliography

Ahlfors, Seppo P, Jooman Han, Fa Hsuan Lin, Thomas Witzel, John W Belliveau, Matti S Hämäläinen, and Eric Halgren. 2010. "Cancellation of EEG and MEG Signals Generated by Extended and Distributed Sources." *Human Brain Mapping* 31 (1). Wiley Subscription Services, Inc., A Wiley Company: 140–49. doi:10.1002/hbm.20851.

Ahlfors, Seppo P, Jooman Han, John W Belliveau, and Matti S Hämäläinen. 2010. "Sensitivity of MEG and EEG to Source Orientation." *Brain Topography* 23 (3): 227–32. doi:10.1007/s10548-010-0154-x.

Astolfi, Laura, Febo Cincotti, Donatella Mattia, M Grazia Marciani, Luiz A Baccala, Fabrizio de Vico Fallani, Serenella Salinari, et al. 2007. "Comparison of Different Cortical Connectivity Estimators for High-Resolution EEG Recordings.." *Human Brain Mapping* 28 (2): 143–57. doi:10.1002/hbm.20263.

Aydin, Ümit, Johannes Vorwerk, Matthias Dümpelmann, Philipp Küpper, Harald Kugel, Marcel Heers, Jörg Wellmer, et al. 2015. "Combined EEG/MEG Can Outperform Single Modality EEG or MEG Source Reconstruction in Presurgical Epilepsy Diagnosis." Edited by Daniele Marinazzo. *Plos One* 10 (3): e0118753–29. doi:10.1371/journal.pone.0118753.

Babiloni, F, F Cincotti, C Babiloni, F Carducci, D Mattia, L Astolfi, A Basilisco, et al. 2005. "Estimation of the Cortical Functional Connectivity with the Multimodal Integration of High-Resolution EEG and fMRI Data by Directed Transfer Function.." *Neuroimage* 24 (1): 118–31. doi:10.1016/j.neuroimage.2004.09.036.

Babiloni, Fabio, Filippo Carducci, Febo Cincotti, Cosimo Del Gratta, Vittorio Pizzella, Gian Luca Romani, Paolo Maria Rossini, Franca Tecchio, and Claudio Babiloni. 2001. "Linear Inverse Source Estimate of Combined EEG and MEG Data Related to Voluntary Movements." *Human Brain Mapping* 14 (4). John Wiley & Sons, Inc.: 197–209. doi:10.1002/hbm.1052.

Baillet, S, and L Garnero. 1997. "A Bayesian Approach to Introducing Anatomo-Functional Priors in the EEG/MEG Inverse Problem." *IEEE Transactions on Biomedical Engineering* 44 (5): 374–85. doi:10.1109/10.568913.

Balish, M, S Sato, P Connaughton, and C Kufta. 1991. "Localization of Implanted Dipoles by Magnetoencephalography." *Neurology*.

Bast, Thomas, Oezdin Oezkan, Sabine Rona, Christoph Stippich, Angelika Seitz, André Rupp, Susanne Fauser, Josef Zentner, Dietz Rating, and Michael Scherg. 2004. "EEG and MEG Source Analysis of Single and Averaged Interictal Spikes Reveals Intrinsic Epileptogenicity in Focal Cortical Dysplasia.." *Epilepsia* 45 (6): 621–31. doi:10.1111/j.0013-9580.2004.56503.x.

Baumgartner, C, G Lindinger, A Ebner, and S Aull. 1995. "Propagation of Interictal Epileptic Activity in Temporal Lobe Epilepsy." *Neurology*.

Bautista, Ramon Edmundo D, Mark A Cobbs, Dennis D Spencer, and Susan S Spencer. 1999. "Prediction of Surgical Outcome by Interictal Epileptiform Abnormalities During Intracranial EEG Monitoring in Patients with Extrahippocampal Seizures." *Epilepsia* 40 (7): 880–90.

doi:10.1111/j.1528-1157.1999.tb00794.x.

Bin He, Lin Yang, C Wilke, and Han Yuan. 2011. “Electrophysiological Imaging of Brain Activity and Connectivity—Challenges and Opportunities.” *IEEE Transactions on Biomedical Engineering* 58 (7): 1918–31. doi:10.1109/TBME.2011.2139210.

Blanke, O, S Morand, G Thut, C M Michel, L Spinelli, T Landis, and M Seeck. 1999. “Visual Activity in the Human Frontal Eye Field.” *NeuroReport* 10 (5): 925–30. doi:10.1097/00001756-199904060-00006.

Brodbeck, Verena, Laurent Spinelli, Agustina M Lascano, Michael Wissmeier, Maria-Isabel Vargas, Serge Vulliemoz, Claudio Pollo, Karl Schaller, Christoph M Michel, and Margitta Seeck. 2011. “Electroencephalographic Source Imaging: a Prospective Study of 152 Operated Epileptic Patients..” *Brain* 134 (Pt 10): 2887–97. doi:10.1093/brain/awr243.

Brookes, Matthew J, Brookes, M J, Mark W Woolrich, M W Woolrich, Darren Price, and D Price. 2014. “An Introduction to MEG Connectivity Measurements.” In *Magnetoencephalography*, 321–58. Berlin, Heidelberg: Springer Berlin Heidelberg. doi:10.1007/978-3-642-33045-2_16.

Chen, Fangmin, Hans Hallez, and Steven Staelens. 2010. “Influence of Skull Conductivity Perturbations on EEG Dipole Source Analysis.” *Medical Physics* 37 (8). American Association of Physicists in Medicine: 4475–84. doi:10.1118/1.3466831.

Chowdhury, Rasheda Arman, Giovanni Pellegrino, Ümit Aydin, Jean-Marc Lina, Francois Dubeau, Eliane Kobayashi, and Christophe Grova. 2017. “Reproducibility of EEG-MEG Fusion Source Analysis of Interictal Spikes: Relevance in Presurgical Evaluation of Epilepsy.” *Human Brain Mapping* 132 (November): 3060. doi:10.1002/hbm.23889.

Chowdhury, Rasheda Arman, Jean-Marc Lina, Eliane Kobayashi, and Christophe Grova. 2013. “MEG Source Localization of Spatially Extended Generators of Epileptic Activity: Comparing Entropic and Hierarchical Bayesian Approaches.” Edited by Gareth Robert Barnes. *Plos One* 8 (2). Public Library of Science: e55969. doi:10.1371/journal.pone.0055969.

Coben, Robert, and Iman Mohammad-Rezazadeh. 2015. “Neural Connectivity in Epilepsy as Measured by Granger Causality..” *Frontiers in Human Neuroscience* 9: 194. doi:10.3389/fnhum.2015.00194.

Cohen, D, and B N Cuffin. 1987. “A Method for Combining MEG and EEG to Determine the Sources.” *Physics in Medicine and Biology* 32 (1). IOP Publishing: 85–89. doi:10.1088/0031-9155/32/1/013.

Cohen, David, and B Neil Cuffin. 1983. “Demonstration of Useful Differences Between Magnetoencephalogram and Electroencephalogram.” *Electroencephalography and Clinical Neurophysiology* 56 (1): 38–51. doi:10.1016/0013-4694(83)90005-6.

Coito, Ana, Melanie Genetti, Francesca Pittau, Giannina R Iannotti, Aljoscha Thomschewski, Yvonne Höller, Eugen Trinka, et al. 2016. “Altered Directed Functional Connectivity in Temporal Lobe Epilepsy in the Absence of Interictal Spikes: a High Density EEG Study.” *Epilepsia* 57 (3): 402–11. doi:10.1111/epi.13308.

Dai, Yakang, Wenbo Zhang, Deanna L Dickens, and Bin He. 2012. “Source Connectivity

Analysis From MEG and Its Application to Epilepsy Source Localization..” *Brain Topography* 25 (2). Springer US: 157–66. doi:10.1007/s10548-011-0211-0.

Dale, A M, and M I Sereno. 1993. “Improved Localizadon of Cortical Activity by Combining EEG and MEG with MRI Cortical Surface Reconstruction: a Linear Approach.” *Journal of Cognitive Neuroscience*.

de Peralta Menendez, R G, and S L Gonzalez-Andino. 1998. “A Critical Analysis of Linear Inverse Solutions to the Neuroelectromagnetic Inverse Problem.” *IEEE Transactions on Biomedical Engineering* 45 (4): 440–48. doi:10.1109/10.664200.

Ding, L, G A Worrell, T D Lagerlund, and B He. 2007. “Ictal Source Analysis: Localization and Imaging of Causal Interactions in Humans.” *Neuroimage*.

Ding, Lei, and Bin He. 2004. “Sparse Source Imaging in EEG.” In, 20–23. IEEE. doi:10.1109/NFSI-ICFBI.2007.4387677.

Ding, Lei, Gregory A Worrell, Terrence D Lagerlund, and Bin He. 2006. “3D Source Localization of Interictal Spikes in Epilepsy Patients with MRI Lesions.” *Physics in Medicine and Biology* 51 (16): 4047–62. doi:10.1088/0031-9155/51/16/011.

Ding, Lei, Guofa Shou, Han Yuan, Diamond Urbano, and Yoon-Hee Cha. 2014. “Lasting Modulation Effects of rTMS on Neural Activity and Connectivity as Revealed by Resting-State EEG..” *IEEE Transactions on Bio-Medical Engineering* 61 (7): 2070–80. doi:10.1109/TBME.2014.2313575.

Ebersole, John S, and Susan M Ebersole. 2010. “Combining MEG and EEG Source Modeling in Epilepsy Evaluations.” *Journal of Clinical Neurophysiology* 27 (6): 360–71. doi:10.1097/WNP.0b013e318201ffc4.

Elisevich, Kost, Neetu Shukla, John E Moran, Brien Smith, Lonni Schultz, Karen Mason, Gregory L Barkley, Norman Tepley, Valentina Gumenyuk, and Susan M Bowyer. 2011. “An Assessment of MEG Coherence Imaging in the Study of Temporal Lobe Epilepsy..” *Epilepsia* 52 (6). Blackwell Publishing Ltd: 1110–19. doi:10.1111/j.1528-1167.2011.02990.x.

Engel, Jerome. 2008. “Surgical Treatment for Epilepsy.” *Jama* 300 (21): 2548. doi:10.1001/jama.2008.756.

England, Mary Jane, Catharyn T Liverman, Andrea M Schultz, and Larisa M Strawbridge. 2012. “Epilepsy Across the Spectrum: Promoting Health and Understanding..” *Epilepsy & Behavior* 25 (2): 266–76. doi:10.1016/j.yebeh.2012.06.016.

FENDER, D H. 1987. “Source Localization of Brain Electrical Activity.” *Methods of Analysis of Brain Electrical and Magnetic Signals*, 355–403.

Fuchs, Manfred, Michael Wagner, Hans-Aloys Wischmann, Thomas Köhler, Annette Theißen, Ralf Drenckhahn, and Helmut Buchner. 1998. “Improving Source Reconstructions by Combining Bioelectric and Biomagnetic Data.” *Electroencephalography and Clinical Neurophysiology* 107 (2): 93–111. doi:10.1016/S0013-4694(98)00046-7.

Gharib, Sina, William W Sutherling, Nobukazu Nakasato, Daniel S Barth, Christoph

Baumgartner, N Alexopoulos, Steve Taylor, and Robert L Rogers. 1995. “MEG and ECoG Localization Accuracy Test.” *Electroencephalography and Clinical Neurophysiology* 94 (2): 109–14. doi:10.1016/0013-4694(94)00276-Q.

Goldenholz, Daniel M, Seppo P Ahlfors, Matti S Hämäläinen, Dahlia Sharon, Mamiko Ishitobi, Lucia M Vaina, and Steven M Stufflebeam. 2009. “Mapping the Signal-to-Noise-Ratios of Cortical Sources in Magnetoencephalography and Electroencephalography.” *Human Brain Mapping* 30 (4). Wiley Subscription Services, Inc., A Wiley Company: 1077–86. doi:10.1002/hbm.20571.

Gonçalves, S I, J C de Munck, J P A Verbunt, F Bijma, R M Heethaar, and F Lopes da Silva. 2003. “In Vivo Measurement of the Brain and Skull Resistivities Using an Eit-Based Method and Realistic Models for the Head.” *IEEE Transactions on Biomedical Engineering* 50 (6): 754–67. doi:10.1109/TBME.2003.812164.

Granger, C W J, and Granger, CWJ. 2001. “Testing for Causality: a Personal Viewpoint.” In *Essays in Econometrics Vol II: Collected Papers of Clive W. J. Granger*, 48–70. New York: Cambridge University Press. doi:10.1017/CCOL052179207X.003.

Grova, C, J Daunizeau, J M Lina, C G Bénar, H Benali, and J Gotman. 2006. “Evaluation of EEG Localization Methods Using Realistic Simulations of Interictal Spikes.” *Neuroimage* 29 (3): 734–53. doi:10.1016/j.neuroimage.2005.08.053.

Hallez, Hans, Bart Vanrumste, Roberta Grech, Joseph Muscat, Wim De Clercq, Anneleen Vergult, Yves D'Asseler, et al. 2007. “Review on Solving the Forward Problem in EEG Source Analysis.” *Journal of NeuroEngineering and Rehabilitation* 4 (1). BioMed Central: 46. doi:10.1186/1743-0003-4-46.

Hara, K, F H Lin, S Camposano, D M Foxe, P E Grant, B F Bourgeois, S P Ahlfors, and S M Stufflebeam. 2007. “Magnetoencephalographic Mapping of Interictal Spike Propagation: a Technical and Clinical Report.” *American Journal of Neuroradiology* 28 (8). American Journal of Neuroradiology: 1486–88. doi:10.3174/ajnr.A0596.

Hämäläinen, M S, and J Sarvas. 1989. “Realistic Conductivity Geometry Model of the Human Head for Interpretation of Neuromagnetic Data.” *IEEE Transactions on Biomedical Engineering* 36 (2): 165–71. doi:10.1109/10.16463.

Hämäläinen, M S, and R J Ilmoniemi. 1994. “Interpreting Magnetic Fields of the Brain: Minimum Norm Estimates.” *Medical and Biological Engineering and ….*

Hämäläinen, Matti, Riitta Hari, Risto J Ilmoniemi, Jukka Knuutila, and Olli V Lounasmaa. 1993. “Magnetoencephalography—Theory, Instrumentation, and Applications to Noninvasive Studies of the Working Human Brain.” *Reviews of Modern Physics* 65 (2). American Physical Society: 413–97. doi:10.1103/RevModPhys.65.413.

He, B, T Musha, Y Okamoto, S Homma, Y Nakajima, and T Sato. 1987. “Electric Dipole Tracing in the Brain by Means of the Boundary Element Method and Its Accuracy..” *IEEE Transactions on Bio-Medical Engineering* 34 (6): 406–14.

He, Bin, Yakang Dai, Laura Astolfi, Fabio Babiloni, Han Yuan, and Lin Yang. 2011. “eConnectome: a MATLAB Toolbox for Mapping and Imaging of Brain Functional

Connectivity..” *Journal of Neuroscience Methods* 195 (2): 261–69. doi:10.1016/j.jneumeth.2010.11.015.

Helmholtz, H. 1853. “Ueber Einige Gesetze Der Vertheilung Elektrischer Ströme in Körperlichen Leitern Mit Anwendung Auf Die Thierisch-Elektrischen Versuche.” *Annalen Der Physik Und Chemie* 165 (6): 211–33. doi:10.1002/andp.18531650603.

Hillebrand, A, and G R Barnes. 2002. “A Quantitative Assessment of the Sensitivity of Whole-Head MEG to Activity in the Adult Human Cortex.” *Neuroimage*.

Huang, M X, T Song, D J Hagler, I Podgorny, and V Jousmaki. 2007. “A Novel Integrated MEG and EEG Analysis Method for Dipolar Sources.” *Neuroimage*.

Hufnagel, A, M Dümpelmann, J Zentner, O Schijns, and C E Elger. 2000. “Clinical Relevance of Quantified Intracranial Interictal Spike Activity in Presurgical Evaluation of Epilepsy.” *Epilepsia* 41 (4): 467–78. doi:10.1111/j.1528-1157.2000.tb00191.x.

Huiskamp, G. 2008. “Interindividual Variability of Skull Conductivity: an EEG-MEG Analysis..” *Analysis*.

Huizenga, H M, T L van Zuijen, D J Heslenfeld, and P C M Molenaar. 2001. “Simultaneous MEG and EEG Source Analysis.” *Physics in Medicine and Biology* 46 (7): 1737–51. doi:10.1088/0031-9155/46/7/301.

Huppertz, H J, S Hoegg, C Sick, C H Lücking, J Zentner, A Schulze-Bonhage, and R Kristeva-Feige. 2001. “Cortical Current Density Reconstruction of Interictal Epileptiform Activity in Temporal Lobe Epilepsy.” *Clinical Neurophysiology* 112 (9): 1761–72. doi:10.1016/S1388-2457(01)00588-0.

Hyvärinen, A, J Karhunen, and E Oja. 2004. *Independent Component Analysis*.

Iwasaki, Masaki, Elia Pestana, Richard C Burgess, Hans O Lüders, Hiroshi Shamoto, and Nobukazu Nakasato. 2005. “Detection of Epileptiform Activity by Human Interpreters: Blinded Comparison Between Electroencephalography and Magnetoencephalography.” *Epilepsia* 46 (1). Blackwell Science Inc: 59–68. doi:10.1111/j.0013-9580.2005.21104.x.

Jie, Biao, Daoqiang Zhang, Wei Gao, Qian Wang, Chong-Yaw Wee, and Dinggang Shen. 2014. “Integration of Network Topological and Connectivity Properties for Neuroimaging Classification..” *IEEE Transactions on Bio-Medical Engineering* 61 (2): 576–89. doi:10.1109/TBME.2013.2284195.

Knake, S, E Halgren, H Shiraishi, K Hara, and H M Hamer. 2006. “The Value of Multichannel MEG and EEG in the Presurgical Evaluation of 70 Epilepsy Patients.” *Epilepsy Research*.

Köhling, R, J M Höhling, H Straub, D Kuhlmann, U Kuhnt, I Tuxhorn, A Ebner, et al. 2000. “Optical Monitoring of Neuronal Activity During Spontaneous Sharp Waves in Chronically Epileptic Human Neocortical Tissue..” *Journal of Neurophysiology* 84 (4): 2161–65.

Krings, Timo, Keith H Chiappa, B Neil Cuffin, Bradley R Buchbinder, and G Rees Cosgrove. 1998. “Accuracy of Electroencephalographic Dipole Localization of Epileptiform Activities Associated with Focal Brain Lesions.” *Annals of Neurology* 44 (1). Wiley Subscription Services,

Inc., A Wiley Company: 76–86. doi:10.1002/ana.410440114.

Lai, Y, W Van Drongelen, L Ding, K E Hecox, V L Towle, D M Frim, and B He. 2005. “Estimation of in Vivo Human Brain-to-Skull Conductivity Ratio From Simultaneous Extra- and Intra-Cranial Electrical Potential Recordings.” *Clinical Neurophysiology* 116 (2): 456–65.

Lantz, G, R Grave de Peralta, L Spinelli, M Seeck, and C M Michel. 2003. “Epileptic Source Localization with High Density EEG: How Many Electrodes Are Needed?.” *Clinical Neurophysiology* 114 (1): 63–69.

Leahy, R M, J C Mosher, M E Spencer, M X Huang, and J D Lewine. 1998. “A Study of Dipole Localization Accuracy for MEG and EEG Using a Human Skull Phantom.” *Electroencephalography and Clinical Neurophysiology* 107 (2): 159–73. doi:10.1016/S0013-4694(98)00057-1.

Lin, Fa Hsuan, John W Belliveau, Anders M Dale, and Matti S Hämäläinen. 2006. “Distributed Current Estimates Using Cortical Orientation Constraints.” *Human Brain Mapping* 27 (1). Wiley Subscription Services, Inc., A Wiley Company: 1–13. doi:10.1002/hbm.20155.

Liu, A K, A M Dale, and J W Belliveau. 2002. “Monte Carlo Simulation Studies of EEG and MEG Localization Accuracy.” *Human Brain Mapping*.

Liu, Aiping, Xiaohui Chen, Z Jane Wang, Qi Xu, Silke Appel-Cresswell, and Martin J McKeown. 2014. “A Genetically Informed, Group FMRI Connectivity Modeling Approach: Application to Schizophrenia..” *IEEE Transactions on Bio-Medical Engineering* 61 (3): 946–56. doi:10.1109/TBME.2013.2294151.

Liu, Ying, Jason Moser, and Selin Aviyente. 2014. “Network Community Structure Detection for Directional Neural Networks Inferred From Multichannel Multisubject EEG Data..” *IEEE Transactions on Bio-Medical Engineering* 61 (7): 1919–30. doi:10.1109/TBME.2013.2296778.

Lu, Y, L Yang, G A Worrell, and B He. 2012. “Seizure Source Imaging by Means of FINE Spatio-Temporal Dipole Localization and Directed Transfer Function in Partial Epilepsy Patients.” *Clinical Neurophysiology*.

Malmivuo, J A, and V Suihko. 2001. “Effect of Skull Resistivity on the Relative Sensitivity Distributions of EEG and MEG Measurements.” In, 1:984–85. IEEE. doi:10.1109/IEMBS.2001.1019118.

Marsh, Eric D, Bradley Peltzer, Merritt W Brown, Courtney Wusthoff, Phillip B Storm, Brian Litt, and Brenda E Porter. 2010. “Interictal EEG Spikes Identify the Region of Electrographic Seizure Onset in Some, but Not All, Pediatric Epilepsy Patients..” *Epilepsia* 51 (4). Blackwell Publishing Ltd: 592–601. doi:10.1111/j.1528-1167.2009.02306.x.

Michel, Christoph M, Göran Lantz, Laurent Spinelli, Rolando Grave De Peralta, Theodor Landis, and Margitta Seeck. 2004. “128-Channel EEG Source Imaging in Epilepsy: Clinical Yield and Localization Precision..” *Journal of Clinical Neurophysiology* 21 (2). Journal of Clinical Neurophysiology: 71–83.

Molins, A, S M Stufflebeam, E N Brown, and M S Hämäläinen. 2008. “Quantification of the Benefit From Integrating MEG and EEG Data in Minimum ℓ2-Norm Estimation.” *Neuroimage*

42 (3): 1069–77. doi:10.1016/j.neuroimage.2008.05.064.

Neil Cuffin, B, and David Cohen. 1979. “Comparison of the Magnetoencephalogram and Electroencephalogram.” *Electroencephalography and Clinical Neurophysiology* 47 (2): 132–46. doi:10.1016/0013-4694(79)90215-3.

Nuwer, M R. 1988. “Quantitative EEG: I. Techniques and Problems of Frequency Analysis and Topographic Mapping..” *Journals.Lww.com*.

Oostendorp, T F, and J Delbeke. 1999. “The Conductivity of the Human Skull in Vivo and in Vitro.” In, 1:456. IEEE. doi:10.1109/IEMBS.1999.802534.

Palmini, Andr, Frederick Andermann, Andr Olivier, Donatella Tampieri, Yvon Robitaille, Eva Andermann, and Geoffrey Wright. 1991. “Focal Neuronal Migration Disorders and Intractable Partial Epilepsy: a Study of 30 Patients.” *Annals of Neurology* 30 (6): 741–49. doi:10.1002/ana.410300602.

Pascual-Marqui, R D. 2002. “Standardized Low-Resolution Brain Electromagnetic Tomography (sLORETA): Technical Details.” *Methods Find Exp Clin Pharmacol*.

Rocca, D La, P Campisi, B Vegso, P Cserti, G Kozmann, F Babiloni, and F De Vico Fallani. 2014. “Human Brain Distinctiveness Based on EEG Spectral Coherence Connectivity..” *IEEE Transactions on Bio-Medical Engineering* 61 (9): 2406–12. doi:10.1109/TBME.2014.2317881.

Said, H. 2001. “A Brief Review on Integrated Audio-Visual Processing for Personal Identification.” In, 1996:4–4. IEE. doi:10.1049/ic:19961148.

Sohrabpour, Abbas, Shuai Ye, Gregory A Worrell, Wenbo Zhang, and Bin He. 2016. “Noninvasive Electromagnetic Source Imaging and Granger Causality Analysis: an Electrophysiological Connectome (eConnectome) Approach.” *IEEE Transactions on Biomedical Engineering* 63 (12): 2474–87. doi:10.1109/TBME.2016.2616474.

Sohrabpour, Abbas, Yunfeng Lu, Gregory Worrell, and Bin He. 2016. “Imaging Brain Source Extent From EEG/MEG by Means of an Iteratively Reweighted Edge Sparsity Minimization (IRES) Strategy.” *Neuroimage* 142 (November): 27–42. doi:10.1016/j.neuroimage.2016.05.064.

Sohrabpour, Abbas, Yunfeng Lu, Pongkiat Kankirawatana, Jeffrey Blount, Hyunmi Kim, and Bin He. 2015. “Effect of EEG Electrode Number on Epileptic Source Localization in Pediatric Patients.” *Clinical Neurophysiology* 126 (3): 472–80. doi:10.1016/j.clinph.2014.05.038.

Staley, Kevin J, and F Edward Dudek. 2006. “Interictal Spikes and Epileptogenesis.” *Epilepsy Currents* 6 (6): 199–202. doi:10.1111/j.1535-7511.2006.00145.x.

Talairach, J, and J Bancaud. 1973. “Stereotaxic Approach to Epilepsy.” In *Progress in Neurological Surgery*, 5:297–354. Progress in Neurological Surgery. Karger Publishers. doi:10.1159/000394343.

Tanaka, Naoaki, and Steven M Stufflebeam. 2014. “Clinical Application of Spatiotemporal Distributed Source Analysis in Presurgical Evaluation of Epilepsy.” *Frontiers in Human Neuroscience* 8: 62. doi:10.3389/fnhum.2014.00062.

Tucker, D M. 1993. “Spatial Sampling of Head Electrical Fields: the Geodesic Sensor Net..” *Electroencephalography and Clinical Neurophysiology* 87 (3): 154–63.

Vallaghé, S, and M Clerc. 2009. “A Global Sensitivity Analysis of Three- and Four-Layer EEG Conductivity Models.” *IEEE Transactions on Biomedical Engineering* 56 (4): 988–95. doi:10.1109/TBME.2008.2009315.

Wang, Defeng, Youyong Kong, Winnie C W Chu, Cindy W C Tam, Linda C W Lam, Yilong Wang, Georg Northoff, Vincent C T Mok, Yongjun Wang, and Lin Shi. 2014. “Generation of the Probabilistic Template of Default Mode Network Derived From Resting-State fMRI..” *IEEE Transactions on Bio-Medical Engineering* 61 (10): 2550–55. doi:10.1109/TBME.2014.2323078.

Wang, G, and D Ren. 2013. “Effect of Brain-to-Skull Conductivity Ratio on EEG Source Localization Accuracy.” *BioMed Research International*.

Wendel, Katrina, Outi Väisänen, Jaakko Malmivuo, Nevzat G Gencer, Bart Vanrumste, Piotr Durka, Ratko Magjarević, et al. 2009. “EEG/MEG Source Imaging: Methods, Challenges, and Open Issues.” *Computational Intelligence and Neuroscience* 2009 (2): 1–12. doi:10.1155/2009/656092.

Yamamoto, T, S J Williamson, L Kaufman, C Nicholson, and R Llinás. 1988. “Magnetic Localization of Neuronal Activity in the Human Brain..” *Proceedings of the National Academy of Sciences* 85 (22). National Acad Sciences: 8732–36.

Zhang, Yingchun, Wim van Drongelen, Bin He. 2006. “Estimation of in Vivo Brain-to-Skull Conductivity Ratio in Humans.” *Applied Physics Letters* 89 (22). American Institute of Physics: 223903. doi:10.1063/1.2398883.